Double-charm heptaquark states composed of two charmed mesons and one nucleon

Si-Qiang Luo,[1,2,3,*] Li-Sheng Geng,[4,5,6,7,†] and Xiang Liu[1,7,3,8,‡]

[1]*School of Physical Science and Technology, Lanzhou University, Lanzhou 730000, China*
[2]*School of Mathematics and Statistics, Lanzhou University, Lanzhou 730000, China*
[3]*Research Center for Hadron and CSR Physics, Lanzhou University and Institute of Modern Physics of CAS, Lanzhou 730000, China*
[4]*School of Physics, Beihang University, Beijing 102206, China*
[5]*Beijing Key Laboratory of Advanced Nuclear Materials and Physics, Beihang University, Beijing 102206, China*
[6]*School of Physics and Microelectronics, Zhengzhou University, Zhengzhou, Henan 450001, China*
[7]*Lanzhou Center for Theoretical Physics, Lanzhou University, Lanzhou 730000, China*
[8]*Key Laboratory of Theoretical Physics of Gansu Province and Frontiers Science Center for Rare Isotopes, Lanzhou University, Lanzhou 730000, China*

(Received 11 June 2022; accepted 13 July 2022; published 22 July 2022)

Inspired by the experimental discoveries of T_{cc}, $\Sigma_c(2800)$, and $\Lambda_c(2940)$ and the theoretical picture where they are DD^*, DN, and D^*N molecular candidates, we investigate the double-charm heptaquark system of DD^*N. We employ the one-boson-exchange model to deduce the pairwise D-D^*, D-N, and D^*-N potentials and then study the DD^*N system with the Gaussian expansion method. We find two good hadronic molecular candidates with $I(J^P) = \frac{1}{2}(\frac{1}{2}^+)$ and $\frac{1}{2}(\frac{3}{2}^+)$ DD^*N with only S-wave pairwise interactions. The conclusion remains unchanged even taking into account the S-D mixing and coupled channel effects. In addition to providing the binding energies, we also calculate the root-mean-square radii of the DD^*N system, which further support the molecular nature of the predicted states. They can be searched for at the upcoming LHC run 3 and run 4.

DOI: 10.1103/PhysRevD.106.014017

I. INTRODUCTION

The precision frontier of particle physics is always full of surprises. With increasing experimental precision, we have had first glimpses of exotic hadronic states. Remarkable progress in identifying new hidden-charm tetraquark states and observing a series of XYZ charmoniumlike states, the P_c pentaquark states [1,2], the hexaquark candidates such as $Y(4630)$ observed in $e^+e^- \to \Lambda_c\bar{\Lambda}_c$ [3], and $d^*(2380)$ [4–9] has been made in the past two decades. Obviously, the study of exotic hadronic states can provide valuable information on understanding the nonperturbative behavior of quantum chromodynamics. We refer interested readers to Refs. [10–17] for comprehensive reviews in this regard.

Conventional mesons and baryons consist of two and three valence quarks. With the increasing number of valence quarks, we are now witnessing the emergence of tetraquark, pentaquark, and heptaquark states. Facing the novel hadronic matter mentioned above and given the exciting experimental observations, one wonders whether or not there exists exotic hadronic matter composed of more valence quarks, and heptaquark states naturally come to our mind (see Fig. 1). Heptaquark states composed of seven quarks are not only a fantastic concept in few-body physics, but also a realistically allowed kind of exotic hadron matter in hadron physics, which deserve to be explored.

Scrutinizing all the newly discovered hadrons, we notice three interesting ones, i.e., T_{cc}^+, $\Lambda_c(2940)$, and $\Sigma_c(2800)$. In 2021, the LHCb Collaboration observed the T_{cc}^+ state in the $D^0D^0\pi^+$ invariant mass spectrum [18,19], which is a good candidate for the $D\bar{D}^*$ molecular state [20–29]. The discovery of the $\Lambda_c(2940)$ was reported by the *BABAR* Collaboration in the D^0p invariant mass spectrum [30] and confirmed in the $\Sigma_c(2455)\pi$ channel by the Belle Collaboration [31] and in the $\Lambda_b^0 \to D^0p\pi^-$ process by the LHCb Collaboration [32]. To understand its low mass, the $\Lambda_c(2940)$ was suggested to be a D^*N molecule [33–37]

*luosq15@lzu.edu.cn
†lisheng.geng@buaa.edu.cn
‡xiangliu@lzu.edu.cn

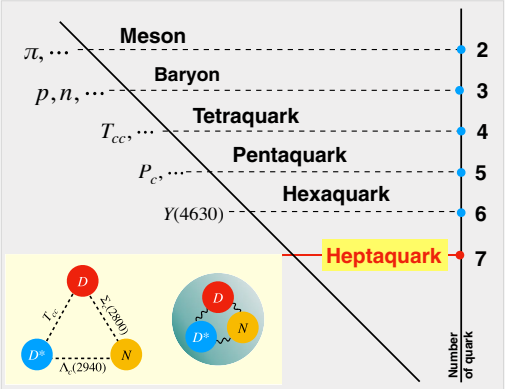

FIG. 1. Emergence of heptaquark states with the increasing number of valence quarks.

or a conventional baryon whose mass is lowered by the strong coupled-channel effect of D^*N [38]. The $\Sigma_c(2800)$ signal was first found by the Belle Collaboration in the $\Sigma_c^+\pi^{\pm,0}$ channels [39], which has also been interpreted as a DN bound state [40–42]. The above experimental and theoretical efforts have deepened our understanding of the relevant $D\bar{D}^*$, D^*N, and DN interactions.

In this work we propose to study the double-charm heptaquark system of D^*DN, which is composed of two charmed mesons and one nucleon as shown in Fig. 1. Intimately related to the observed T_{cc}^+, $\Lambda_c(2940)$, and $\Sigma_c(2800)$ states, the open-charm heptaquark is an ideal platform to manifest how the change of the DD^*, D^*N, and DN interactions affects the existence of an open-charm heptaquark state. The open-charm heptaquark state is a typical few-body system, where the key issue is to deal with the sub-two-body interactions of the D^*DN system. For this purpose, we adopt the Gaussian expansion method (GEM) [43,44], which is a powerful tool in studying few-body problems. Finally, the spectroscopy of the double-charm heptaquark states can be predicted.

This paper is organized as follows. After the Introduction, we briefly introduce the D-$D^{(*)}$ and $D^{(*)}$-N potentials and the Gaussian expansion method in Sec. II. Then, in Sec. III, we present the binding energies and root-mean-square radii of the DD^*N molecular candidates. We also study the sensitivity of the bound-state solutions to the coupling constants of the potentials in Sec. IV. This paper ends with a short summary in Sec. V.

II. FORMALISM

To study the DD^*N three-body problem, we should first determine the DD^*, DN, and D^*N interactions. Fortunately, the observed T_{cc}^+, $\Lambda_c(2940)$, and $\Sigma_c(2800)$ have simulated studies of the DD^* [20–25], DN [40–42], and D^*N [33] interactions, respectively. In general, the one-boson-exchange (OBE) model provides a realistic framework where the effective interactions between hadron pairs can be deduced. First, we provide the following OBE effective potentials for the $D^{(*)}D^*$ system [27,28,35,45]:

$$\begin{aligned}
V^{DD^*\to DD^*} &= -g_\sigma^2\mathcal{O}_1 Y_\sigma + \frac{1}{2}\beta^2 g_V^2\mathcal{O}_1\mathcal{H}_V,\\
V^{DD^*\to D^*D} &= \frac{g^2}{3f_\pi^2}(\mathcal{O}_2\hat{\mathcal{O}}+\mathcal{O}_3\hat{\mathcal{P}})\mathcal{H}'_{P1} + \frac{2}{3}\lambda^2 g_V^2(2\mathcal{O}_2\hat{\mathcal{O}}-\mathcal{O}_3\hat{\mathcal{P}})\mathcal{H}'_{V1},\\
V^{DD^*\to D^*D^*} &= \frac{g^2}{3f_\pi^2}(\mathcal{O}_4\hat{\mathcal{O}}+\mathcal{O}_5\hat{\mathcal{P}})\mathcal{H}_{P2} + \frac{2}{3}\lambda^2 g_V^2(2\mathcal{O}_4\hat{\mathcal{O}}-\mathcal{O}_5\hat{\mathcal{P}})\mathcal{H}_{V2}.
\end{aligned} \tag{1}$$

For the interactions of $D^{(*)}$-N, we have

$$\begin{aligned}
V^{DN\to DN} &= g_{\sigma NN}g_\sigma\left(1-\frac{\boldsymbol{\sigma}\cdot\mathbf{L}}{4m_N^2}\hat{\mathcal{Q}}\right)Y_\sigma + \left[-h_{vNN}\beta g_V - \frac{(h_{vNN}+2f_{vNN})\beta g_V}{8m_N^2}(\hat{\mathcal{P}}+2\boldsymbol{\sigma}\cdot\mathbf{L}\hat{Q})\right]\mathcal{H}''_V,\\
V^{DN\to D^*N} &= \frac{g_{\pi NN}g_\pi}{3\sqrt{2}m_N f_\pi}(\mathcal{O}_6\hat{\mathcal{O}}+\mathcal{O}_7\hat{\mathcal{P}})\mathcal{H}''_{P3} + \left[-\frac{2h_{vNN}\lambda g_V}{m_N}\mathcal{O}_8\hat{\mathcal{Q}} + \frac{(h_{vNN}+f_{vNN})\lambda g_V}{3m_N}(2\mathcal{O}_6\hat{\mathcal{O}}-\mathcal{O}_7\hat{\mathcal{P}})\right]\mathcal{H}''_{V3},\\
V_{D^*N\to D^*N} &= g_{\sigma NN}g_\sigma\mathcal{O}_9\left(1-\frac{\boldsymbol{\sigma}\cdot\mathbf{L}}{4m_N^2}\hat{\mathcal{Q}}\right)Y_\sigma + \left[-h_{vNN}\beta g_V\mathcal{O}_9 - \frac{(h_{vNN}+2f_{vNN})\beta g_V}{8m_N^2}\mathcal{O}_9(\hat{\mathcal{P}}+2\boldsymbol{\sigma}\cdot\mathbf{L}\hat{Q})\right]\mathcal{H}''_V\\
&\quad + \frac{g_{\pi NN}g_\pi}{3\sqrt{2}m_N f_\pi}(\mathcal{O}_{10}\hat{\mathcal{O}}+\mathcal{O}_{11}\hat{\mathcal{P}})\mathcal{H}''_P + \left[-\frac{2h_{vNN}\lambda g_V}{3m_N}\mathcal{O}_{12}\hat{\mathcal{Q}} + \frac{(h_{vNN}+f_{vNN})\lambda g_V}{3m_N}(2\mathcal{O}_{10}\hat{\mathcal{O}}-\mathcal{O}_{11}\hat{\mathcal{P}})\right]\mathcal{H}''_V.
\end{aligned} \tag{2}$$

In Eqs. (1) and (2), the $\mathcal{O}_i$'s are spin-dependent operators, which read explicitly

$$\begin{aligned}
&\mathcal{O}_1 = \boldsymbol{\epsilon}_4^\dagger \cdot \boldsymbol{\epsilon}_2, \\
&\mathcal{O}_2 = \boldsymbol{\epsilon}_3^\dagger \cdot \boldsymbol{\epsilon}_2, \qquad \mathcal{O}_3 = S(\mathbf{r}, \boldsymbol{\epsilon}_3^\dagger, \boldsymbol{\epsilon}_2), \\
&\mathcal{O}_4 = \boldsymbol{\epsilon}_3^\dagger \cdot (i\boldsymbol{\epsilon}_4^\dagger \times \boldsymbol{\epsilon}_2), \qquad \mathcal{O}_5 = S(\mathbf{r}, \boldsymbol{\epsilon}_3^\dagger, i\boldsymbol{\epsilon}_4^\dagger \times \boldsymbol{\epsilon}_2), \\
&\mathcal{O}_6 = \boldsymbol{\epsilon}_3^\dagger \cdot \boldsymbol{\sigma}, \qquad \mathcal{O}_7 = S(\mathbf{r}, \boldsymbol{\epsilon}_3^\dagger, \boldsymbol{\sigma}), \qquad \mathcal{O}_8 = \boldsymbol{\epsilon}_3^\dagger \cdot \mathbf{L}, \\
&\mathcal{O}_9 = \boldsymbol{\epsilon}_3^\dagger \cdot \boldsymbol{\epsilon}_1, \qquad \mathcal{O}_{10} = i\boldsymbol{\epsilon}_3^\dagger \times \boldsymbol{\epsilon}_1 \cdot \boldsymbol{\sigma}, \\
&\mathcal{O}_{11} = S(\mathbf{r}, i\boldsymbol{\epsilon}_3^\dagger \times \boldsymbol{\epsilon}_1, \boldsymbol{\sigma}), \qquad \mathcal{O}_{12} = i\boldsymbol{\epsilon}_3^\dagger \times \boldsymbol{\epsilon}_1 \cdot \mathbf{L}, \qquad (3)
\end{aligned}$$

where $S(\mathbf{r}, \mathbf{a}, \mathbf{b}) = 3(\mathbf{a} \cdot \hat{\mathbf{r}})(\mathbf{b} \cdot \hat{\mathbf{r}}) - \mathbf{a} \cdot \mathbf{b}$ and $\mathbf{L}$ are tensor and orbital angular momentum operators, respectively. The $\boldsymbol{\epsilon}_i$ $(i = 1, 2)$ and $\boldsymbol{\epsilon}_i^\dagger$ $(i = 3, 4)$ are initial and final polarization vectors of the D^* mesons, respectively. The conjugated potentials of Eqs. (1) and (2) could be obtained by the following interchange of polarization vectors:

$$\boldsymbol{\epsilon}_1 \leftrightarrow \boldsymbol{\epsilon}_3^\dagger, \qquad \boldsymbol{\epsilon}_2 \leftrightarrow \boldsymbol{\epsilon}_4^\dagger. \qquad (4)$$

The $\mathcal{H}_{Pi}^{(\prime,\prime\prime)}$ and $\mathcal{H}_{Vi}^{(\prime,\prime\prime)}$ are defined as

$$\begin{aligned}
\mathcal{H}_{Pi}^{(\prime,\prime\prime)} &= \mathcal{C}_1^{(\prime,\prime\prime)}(I) Y_{\pi i} + \frac{1}{3}\mathcal{C}_0^{(\prime,\prime\prime)}(I) Y_{\eta i}, \\
\mathcal{H}_{Vi}^{(\prime,\prime\prime)} &= \mathcal{C}_1^{(\prime,\prime\prime)}(I) Y_{\rho i} + \mathcal{C}_0^{(\prime,\prime\prime)}(I) Y_{\omega i}, \qquad (5)
\end{aligned}$$

respectively. In Eq. (5), the function Y_i is written as

$$Y_i = \frac{e^{-m_{Ei} r}}{4\pi r} - \frac{e^{-\Lambda_i r}}{4\pi r} - \frac{\Lambda_i^2 e^{-\Lambda_i r}}{8\pi\Lambda_i} + \frac{m_{Ei}^2 e^{-\Lambda_i r}}{8\pi\Lambda_i}, \qquad (6)$$

with $\Lambda_i = \sqrt{\Lambda^2 - q_i^2}$ and $m_{Ei} = \sqrt{m_E^2 - q_i^2}$. The Λ, m_E, and q_i are the cutoff of the monopole form factor $\mathcal{F}(q^2, m_E^2) = (\Lambda^2 - m_E^2)/(\Lambda^2 - q^2)$, the mass of the exchanged meson, and the energy component of the exchanged momentum. The values of q_i $(i = 1, 2, 3)$ are taken as $q_1 = m_{D^*} - m_D$, $q_2 = (m_{D^*}^2 - m_D^2)/(4m_{D^*})$, and $q_3 = (m_{D^*}^2 - m_D^2)/(2(m_{D^*} + m_N))$. The isospin factors $\mathcal{C}^{(\prime,\prime\prime)}(I)$ are

$$\begin{aligned}
&\mathcal{C}_1(0) = -\frac{3}{2}, \quad \mathcal{C}_1'(0) = +\frac{3}{2}, \quad \mathcal{C}_1''(0) = +\frac{3}{2}, \\
&\mathcal{C}_1(1) = +\frac{1}{2}, \quad \mathcal{C}_1'(1) = +\frac{1}{2}, \quad \mathcal{C}_1''(1) = -\frac{1}{2}, \\
&\mathcal{C}_0(0) = +\frac{1}{2}, \quad \mathcal{C}_0'(0) = -\frac{1}{2}, \quad \mathcal{C}_0''(0) = +\frac{1}{2}, \\
&\mathcal{C}_0(1) = +\frac{1}{2}, \quad \mathcal{C}_0'(1) = +\frac{1}{2}, \quad \mathcal{C}_0''(1) = +\frac{1}{2}. \qquad (7)
\end{aligned}$$

The operators $\hat{\mathcal{O}}$, $\hat{\mathcal{P}}$, and $\hat{\mathcal{Q}}$ are defined by

TABLE I. Values of the coupling constants [28,35] and meson masses [46]. The signs are determined by the quark model.

Coupling constants		Meson masses (GeV)	
$\frac{g}{f_\pi} = 4.545\ \mathrm{GeV}^{-1}$	$g_{\pi NN} = -13.07$	$m_\pi = 0.140$	$m_\eta = 0.548$
$g_\sigma = 0.76$	$g_{\sigma NN} = -8.46$	$m_\sigma = 0.600$	$m_D = 1.867$
$\beta g_V = 5.2$	$h_{VNN} = 3.25$	$m_\rho = 0.770$	$m_{D^*} = 2.009$
$\lambda g_V = 3.133\ \mathrm{GeV}^{-1}$	$f_{VNN} = 19.83$	$m_\omega = 0.780$	$m_N = 0.939$

$$\hat{\mathcal{O}} = \frac{1}{r^2}\frac{\partial}{\partial r} r^2 \frac{\partial}{\partial r}, \quad \hat{\mathcal{P}} = r\frac{\partial}{\partial r}\frac{1}{r}\frac{\partial}{\partial r}, \quad \hat{\mathcal{Q}} = \frac{1}{r}\frac{\partial}{\partial r}. \qquad (8)$$

To evaluate the above potentials, we need the values of the coupling constants and the masses of the mesons, which are collected in Table I.

To solve the three-body Schrödinger equation, we employ the GEM [43,44]. It is a popular method widely used in studying multibody hadronic molecular states [25,47–53]. The Jacobi coordinates of the DD^*N system are presented in Fig. 2.

The three-body Schrödinger equation reads

$$\hat{H}\Psi_{JM} = E\Psi_{JM}, \qquad (9)$$

with

$$\hat{H} = \hat{T} + V(r_1) + V(r_2) + V(r_3). \qquad (10)$$

Ψ_{JM} is the total wave function, which is composed of three channels

$$\Psi_{JM} = \sum_{c,\alpha} C_{c,\alpha} H_{t,T}^c [\chi_{s,S}^c [\phi_{nl}(\mathbf{r}_c)\phi_{NL}(\mathbf{R}_c)]_\lambda]_{JM}, \qquad (11)$$

where the coefficient $C_{c,\alpha}$ is determined by the Rayleigh-Ritz variational method. The c $(c = 1, 2, 3)$ represents the three channels in Fig. 2 and $\alpha = \{tT, sS, nN, lL\lambda\}$ are the quantum numbers of the basis. The $H_{t,T}^c$, χ_{s,S,M_S}^c, and $[\phi_{nl}(\mathbf{r}_c)\phi_{NL}(\mathbf{R}_c)]_\lambda$ are flavor, spin, and spatial wave functions, respectively. The $\phi_{nlm_l}(\mathbf{r}_c)$ and $\phi_{NLM_L}(\mathbf{R}_c)$ read

$$\begin{aligned}
\phi_{nlm_l}(\mathbf{r}_c) &= N_{nl} r_c^l e^{-\nu_n r_c^2} Y_{lm}(\hat{\mathbf{r}}_c), \\
\phi_{NLM_L}(\mathbf{R}_c) &= N_{NL} R_c^L e^{-\lambda_N R_c^2} Y_{LM}(\hat{\mathbf{R}}_c), \qquad (12)
\end{aligned}$$

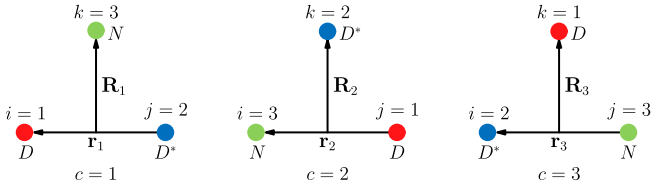

FIG. 2. Jacobi coordinates of the DD^*N system.

TABLE II. Bound-state solutions of the DD^*N system. The cutoff Λ, binding energies E, and root-mean-square radii are in units of GeV, MeV, and femtometer, respectively. The probabilities of DD^*N and D^*D^*N components are presented in the last two rows.

		S wave					S-D mixing effect					Coupled-channel effect			
I	J^P	Λ	E	r_{DD^*}	r_{DN}	r_{D^*N}	Λ	E	r_{DD^*}	r_{DN}	r_{D^*N}	Λ	E	P_{DD^*N} (%)	$P_{D^*D^*N}$ (%)
$\frac{1}{2}$	$\frac{1}{2}^+$	1.19	−0.11	4.31	10.24	10.20	1.02	−1.13	11.64	11.75	2.40	1.00	−0.41	97.75	2.25
		1.24	−2.35	2.10	8.55	8.54	1.07	−21.19	11.56	11.59	1.26	1.05	−11.40	99.98	0.02
		1.29	−6.62	1.38	6.34	6.33	1.12	−56.46	11.55	11.57	0.98	1.10	−40.43	∼100	∼0
	$\frac{3}{2}^+$	1.20	−0.37	3.81	10.24	10.18	0.89	−0.19	9.77	10.22	4.82	0.89	−0.22	99.98	0.02
		1.25	−2.83	1.99	9.51	9.50	0.94	−3.25	9.22	9.34	2.47	0.94	−3.32	99.96	0.04
		1.30	−7.12	1.37	9.13	9.12	0.99	−9.25	9.00	9.05	1.69	0.99	−9.44	99.83	0.17
$\frac{3}{2}$	$\frac{1}{2}^+$	1.84	−0.11	10.71	11.12	5.17	1.77	−0.18	9.86	10.25	4.61	1.77	−0.21	99.99	0.01
		1.89	−0.77	10.43	10.67	3.77	1.82	−0.94	9.63	9.85	3.47	1.82	−0.98	99.98	0.02
		1.94	−1.72	10.24	10.38	2.87	1.87	−1.99	9.45	9.59	2.70	1.87	−2.04	99.98	0.02
	$\frac{3}{2}^+$	2.56	−1.32	2.13	9.01	9.00	1.90	−0.18	14.00	14.21	3.66	1.90	−0.18	∼100	∼0
		2.61	−17.07	0.68	8.59	8.59	1.95	−1.16	13.77	13.90	2.82	1.95	−1.16	∼100	∼0
		2.66	−41.08	0.47	8.53	8.53	2.00	−2.44	13.65	13.73	2.26	2.00	−2.44	∼100	∼0

where N_{nl} and N_{NL} are normalization constants. In Eq. (12), $\mathbf{r}_c$ and $\mathbf{R}_c$ are Jacobi coordinates, and ν_n and λ_N are Gaussian ranges, i.e.,

$$\nu_n = 1/r_n^2, \quad r_n = r_1 a^{n-1} \quad (n = 1,2\cdots n_{\max}),$$
$$\lambda_N = 1/R_N^2, \quad R_N = R_1 A^{N-1} \quad (N = 1,2\cdots N_{\max}). \tag{13}$$

With the above wave functions, all the Hamilton matrix elements could be expressed in simple forms. The details could be found in our previous work [53].

III. NUMERICAL RESULTS

With the deduced potentials, one could search for bound-state solutions with the three-body Schrödinger equation. Before showing the numerical results, we would like to emphasize the following points[1]:

1. The kinetic energy operator is equivalent to a repulsive potential. In general, it is difficult to form a higher partial wave hadronic molecular state. But a three-body system contains two spatial degrees of freedom, and the S-D mixing effects introduce more bases and may affect the numerical results. Thus, in this work, we first consider the S-wave-only scheme. Then, the S-D mixing effects are included.
2. In the S-D mixing scheme, the tensor and spin-orbit terms can contribute to the matrix elements, which should also be taken into account for completeness.
3. In our study, the cutoff Λ is a crucial parameter in determining the existences of bound-state solutions. In our previous works [27,45,54–57], the cutoff Λ is suggested to be about 1 GeV, whose value is supported by the studies of typical hadronic molecular candidates, such as deuteron [57], P_c [54,55], and T_{cc} [25]. If a bound-state solution is obtained with $\Lambda \approx 1$ GeV, this state could be viewed as a good molecular candidate.
4. In our study, the spatial wave functions of D, D^*, and N are not considered. We employ the center of mass of each hadron as the position in the Jacobi coordinates as depicted in Fig. 2. An ideal molecular candidate is that in which the two constituent hadrons should not overlap too much in the spatial distributions. Thus, the root-mean-square radii that describe the sizes of the D, D^*, N, and the three-body molecular states are important parameters when finding out the bound-state solutions. With the Godfrey-Isgur [58] and Capstick-Isgur [59] models, the root-mean-square radii of D, D^*, and N could be estimated to be $r_D \approx 0.40$, $r_{D^*} \approx 0.46$, and $r_N \approx 0.70$ fm, respectively. In this work, we not only present the binding energies, but also calculate the root-mean-square radii between each pair of the three constituents, i.e., r_{DD^*}, r_{DN}, and r_{D^*N}. For a good candidate of molecular state, we expect that there exist the relations $r_{DD^*} \gtrsim r_D + r_{D^*}$, $r_{DN} \gtrsim r_D + r_N$, and $r_{D^*N} \gtrsim r_{D^*} + r_N$ associated with the bound-state solutions.

The numerical results are presented in Table II. We note that it is easy to obtain a bound $I(J^P) = \frac{1}{2}(\frac{1}{2}^+)$ DD^*N state. According to Table II, we can deduce the following:

1. There exist bound-state solutions in the S-wave $I(J^P) = \frac{1}{2}(\frac{1}{2}^+)$ DD^*N configuration for a cutoff $\Lambda \approx 1.2$ GeV. The root-mean-square radii of DD^*, DN, and D^*N are about 3.5, 9, and 9 fm, respectively. Since the cutoff is approximately 1 GeV and the root-mean-square radii are several femtometers, the S-wave $I(J^P) = \frac{1}{2}(\frac{1}{2}^+)$ DD^*N

[1]These are relevant not only to studies of two-body hadronic molecular candidates, but also to those of three-body hadronic molecules.

bound state can be viewed as a good molecular candidate.

2. In the S-D mixing and coupled-channel schemes, there exist as well bound-state solutions for a cutoff $\Lambda \approx 1$ GeV. We note that these effects increase the strength of the attractive potentials such that a smaller cutoff is needed to yield the same binding energies as those of the S-wave-only scheme. Similar phenomena have been observed in Refs. [60–63].

For the S-wave $I(J^P) = \frac{1}{2}(\frac{3}{2}^+)$ DD^*N configuration, we find bound-state solutions when the cutoff Λ is approximately 1.20 GeV. The root-mean-square radii of DD^*, DN, and D^*N are several femtometers. Thus, the S-wave $I(J^P) = \frac{1}{2}(\frac{3}{2}^+)$ DD^*N bound state is also a good molecular candidate. By decomposing the S-wave $I(J^P) = \frac{1}{2}(\frac{3}{2}^+)$ DD^*N configuration, we find an important D^*N substructure with $I(J^P) = 0(\frac{3}{2}^+)$, which could be related to the hadronic molecular candidate $\Lambda_c(2940)$. According to the coupling constant determined in the quark model, the pion exchange interaction of $I(J^P) = 0(\frac{3}{2}^+)D^*N$ is attractive, but repulsive for the $I = 1$ configuration. Therefore, $\Lambda_c(2940)$ is good candidate for a $I(J^P) = 0(\frac{3}{2}^+)D^*N$ molecular state.

When we consider the S-D mixing effect, we find a loosely DD^*N bound state of $I(J^P) = \frac{1}{2}(\frac{3}{2}^+)$ for a $\Lambda \approx 0.89$ GeV. But the coupled-channel effect only plays a minor role in this case, which is manifested by the small fractions of the D^*D^*N component.

In our previous three-body studies of the $D^{(*)}D^{(*)}D^*$ systems, we showed that the systems with higher isospins are much more difficult to bind than the systems of lower isospins, regardless of whether one considers only S-wave interactions, S-D mixings, or coupled-channel effects. The same can be said about the DD^*N system.

For the S-wave $I(J^P) = \frac{3}{2}(\frac{1}{2}^+)$ DD^*N configuration, we obtain bound-state solutions for a cutoff $\Lambda \approx 1.85$ GeV, which is larger than that in the scenarios of $I(J^P) = \frac{1}{2}(\frac{1}{2}^+)$, $\frac{1}{2}(\frac{3}{2}^+)$. The larger cutoff needed or the weaker interaction for isospin $3/2$ can be attributed to the following two factors:

(i) The pion exchange potentials of $1(1^+)$ DD^* and $1(\frac{3}{2}^-)D^*N$ are repulsive.

(ii) The attractiveness of the $I(J^P) = 1(\frac{1}{2}^-)$ DN configuration is also weaker than the $I = 0$ configuration.

When the S-D mixing and coupled-channel effects are included, the cutoff needed to yield loosely bound-state solutions is decreased to $\Lambda \approx 1.77$ GeV

Among the four states, the $I(J^P) = \frac{3}{2}(\frac{3}{2}^-)$ DD^*N configuration is the most difficult to form a bound state, which is reflected by the large cutoff Λ in Table II and Fig. 3. In the S-wave-only scheme, bound-state solutions start to emerge as the cutoff reaches about 2.56 GeV, which is much larger than that of the $I = \frac{1}{2}$ configuration. When the S-D mixing and coupled-channel effects are taken into account, the value of the cutoff Λ decreases to about 1.90 GeV.

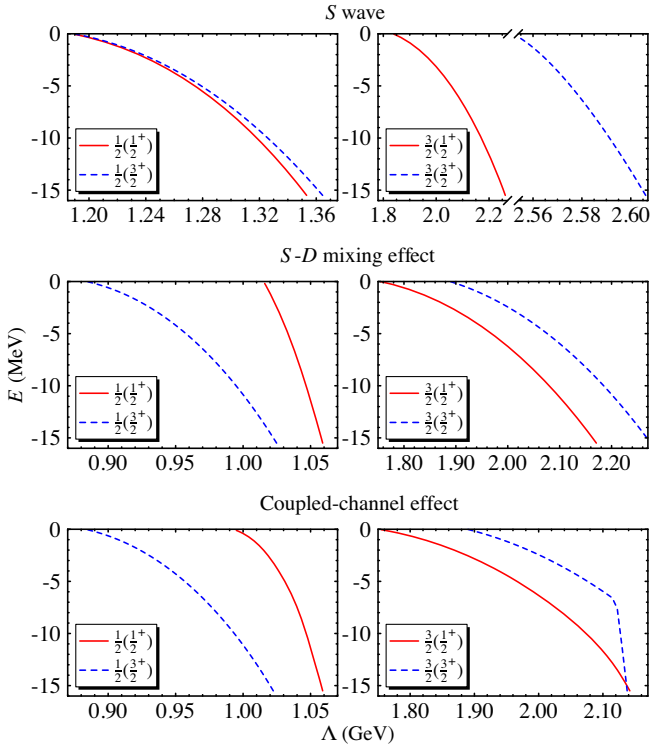

FIG. 3. Binding energies E as functions of the cutoff Λ.

Searching for the predicted DD^*N molecular candidates is a challenging issue. We spell out the isospin wave functions for the convenience of the following discussions. For the DD^*N system with $I = \frac{1}{2}$, its isospin wave function $|I_{DD^*}, I, I_3\rangle$ reads as

$$\begin{aligned}
\left|0,\frac{1}{2},+\frac{1}{2}\right\rangle &= \frac{1}{\sqrt{2}}D^0D^{*+}p - \frac{1}{\sqrt{2}}D^+D^{*0}p,\\
\left|0,\frac{1}{2},-\frac{1}{2}\right\rangle &= \frac{1}{\sqrt{2}}D^0D^{*+}n - \frac{1}{\sqrt{2}}D^+D^{*0}n,\\
\left|1,\frac{1}{2},+\frac{1}{2}\right\rangle &= \frac{1}{\sqrt{6}}D^0D^{*+}p + \frac{1}{\sqrt{6}}D^+D^{*0}p + \sqrt{\frac{2}{3}}D^+D^{*+}n,\\
\left|1,\frac{1}{2},-\frac{1}{2}\right\rangle &= \frac{1}{\sqrt{6}}D^0D^{*+}n + \frac{1}{\sqrt{6}}D^+D^{*0}n + \sqrt{\frac{2}{3}}D^0D^{*0}p.
\end{aligned} \tag{14}$$

And the isospin wave functions of the DD^*N system with $I = \frac{3}{2}$ are

$$\left|1,\frac{3}{2},+\frac{3}{2}\right\rangle = D^{+}D^{*+}p,$$
$$\left|1,\frac{3}{2},+\frac{1}{2}\right\rangle = \frac{1}{\sqrt{3}}D^{0}D^{*+}p+\frac{1}{\sqrt{3}}D^{+}D^{*0}p-\frac{1}{\sqrt{3}}D^{+}D^{*+}n,$$
$$\left|1,\frac{3}{2},-\frac{1}{2}\right\rangle = \frac{1}{\sqrt{3}}D^{0}D^{*0}p+\frac{1}{\sqrt{3}}D^{0}D^{*+}n-\frac{1}{\sqrt{3}}D^{+}D^{*0}n,$$
$$\left|1,\frac{3}{2},-\frac{3}{2}\right\rangle = D^{0}D^{*0}n. \quad (15)$$

By Eqs. (14) and (15), the $I=\frac{1}{2}$ and $I=\frac{3}{2}$ DD^*N systems contain singly and doubly charged states, while the $I=\frac{3}{2}$ DD^*N systems also contain a triply charged state and a neutral state. In this scheme, the triply charged and neutral channels are special when discussing decays of the $I=\frac{3}{2}$ DD^*N states.

In general, the three-body molecular states have abundant decay channels. In this work, we mainly discuss those channels that are both kinematically and Okubo-Zweig-Iizuka allowed, which are summarized as follows:

1. If the DD^*N molecular states have extremely shallow binding energies, they may decay into $T_{cc}^{+}p$. Then, the T_{cc}^{+} could be observed in the $D^0D^0\pi^+$ or $D^0D^+\gamma$ final states. On the other hand, both the theoretical studies [21,27,28] and experimental analyses [19] imply that the T_{cc}^{+} has $I=0$. Thus, the total isospin of the $T_{cc}^{+}p$ channel is $1/2$. If the DD^*N molecular state can be found in the $T_{cc}^{+}p$ channel, this DD^*N molecular state must have $I=1/2$.
2. If the threshold of the $T_{cc}^{+}p$ channel is higher than the masses of the DD^*N molecular states, the $T_{cc}^{+}p$ is kinematically forbidden. Since the D^* mass is about 140 MeV higher than that of the D meson, the DD^*N molecular states may decay into DDp, $DD\pi p$, and $DD\gamma p$.
3. In 2017, the doubly charmed baryon Ξ_{cc}^{++} was observed by the LHCb Collaboration [64]. The thresholds of the $\Xi_{cc}^{++}\pi$ and $\Xi_{cc}^{++}\pi\pi$ channels are about 3760 and 3900 MeV, respectively, which are below the masses of the DD^*N molecular states, which have masses of about 4818 MeV. Obviously, searching for the neutral DD^*N molecular state and single, double, and triple charged DD^*N molecular states by these $\Xi_{cc}^{++}\pi^-\pi^-$, $\Xi_{cc}^{++}\pi^-$, $\Xi_{cc}^{++}\pi^+\pi^-$, and $\Xi_{cc}^{++}\pi^+$ decay channels, respectively, are possible.
4. For the discussed DD^*N molecular system, the $D^{(*)+}p$ and $D^{(*)0}n$ components could annihilate into charmed baryons Σ_c^{++} and Σ_c^0, respectively, while the $D^{(*)0}p$ component can couple with both Σ_c^+ and Λ_c^+. As a result, the DD^*N molecular states may decay into a singly charmed baryon together with a D meson. Because of the isospin conservation, the $I=\frac{1}{2}$ DD^*N molecular states can decay into $\Lambda_cD^{(*)}$ and $\Sigma_c^{(*)}D^{(*)}$, while the $I=\frac{3}{2}$ states can only decay into $\Sigma_c^{(*)}D^{(*)}$. Considering that the $\Lambda_cD^{(*)}$ channels have $I=\frac{1}{2}$, the $\Lambda_cD^{(*)}$ channels are crucial to distinguish the isospins of the DD^*N molecular states. As shown above, the $I=\frac{1}{2}$ systems are much easier to form bound states than the $I=\frac{1}{2}$ systems. We suggest to search for the DD^*N molecular states via the $\Lambda_cD^{(*)}$ channels. In addition, the DD^*N molecular states with $I=\frac{3}{2}$ have typical decay channels $\Sigma_c^{++}D^{(*)+}$ and $\Sigma_c^0D^{(*)0}$.

IV. SENSITIVITIES OF BOUND-STATE SOLUTIONS TO THE COUPLING CONSTANTS

In the previous section, we studied the dependence of binding energies on the cutoff Λ. However, the cutoff Λ is not the only parameter in our study. The coupling constants are also crucial for the existences of bound states. There are eight coupling constants in our OBE potentials, i.e., g/f_π, g_σ, βg_V, λg_V, $g_{\pi NN}$, $g_{\sigma NN}$, h_{VNN}, and f_{VNN}. With the experimental partial decay width of $D^*\to D\pi$, we obtain $g/f_\pi=4.545$ GeV^{-1}, which is close to the value $\frac{g}{f_\pi}=-\frac{3g_{\pi NN}}{5\sqrt{2}m_N}=5.905$ GeV^{-1} determined in the quark model. In addition, the $\beta g_V=5.2$ used in this work is approximate to the quark model result $g_V=2h_{vNN}=6.50$. However, $g_\sigma=0.76$ and $\lambda g_V=3.13$ GeV^{-1} are much less than the quark model results $g_\sigma=-\frac{1}{3}g_{\sigma NN}=2.82$ and $\lambda g_V=\frac{3(f_{VNN}+h_{VNN})}{10m_N}=7.37$ GeV^{-1}.

Since there are eight coupling constants, it is difficult to vary them simultaneously to study the impact on the three-body results. A more appropriate approach is to vary one coupling constant while fixing the remaining and then search for bound states. As discussed in the last paragraph, the values g/f_π and βg_V are consistent with the quark model predictions from $g_{\pi NN}$ and h_{VNN}, respectively. In this sense, the values of g/f_π, βg_V, $g_{\pi NN}$, and h_{VNN} are reasonable, whereas g_σ, λg_V, $g_{\sigma NN}$, and f_{VNN} need to be better understood. Thus, we mainly discuss the sensitivities of bound-state solutions to g_σ, λg_V, $g_{\sigma NN}$, and f_{VNN}.

In this work, we scan g_σ, λg_V, $g_{\sigma NN}$, and f_{VNN} in the range of 0.5–2.0 times the values in Table I. Then we search for the minimum cutoff Λ allowing for bound-state solutions. The numerical results are presented in Fig. 4.

For the $I(J^P)=\frac{1}{2}(\frac{1}{2}^+)$ and $I(J^P)=\frac{1}{2}(\frac{3}{2}^+)$ DD^*N configurations, we find that the minimum Λ is in the range of 1.05–1.20 GeV for the existence of bound-state solutions. This implies that the $I=\frac{1}{2}$ DD^*N states are robust hadronic candidates even if the coupling constants g_σ, λg_V, $g_{\sigma NN}$, and f_{VNN} are allowed to vary by 100% from their central values given in Table I.

For the two $I=\frac{3}{2}$ configuration, the existence of bound-state solutions are much more sensitive to the coupling

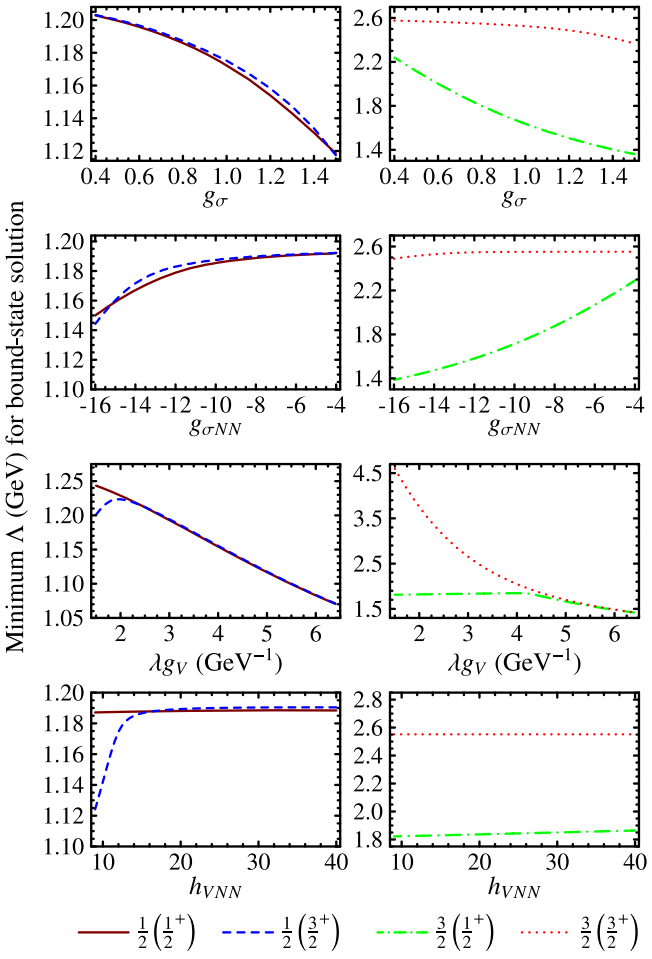

FIG. 4. Dependence of the minimum cutoff Λ on the coupling constants.

constants. From the second column of Fig. 4, we can read the following:

1. If we enlarge the interaction strength of the σ exchange, it is possible to find bound-state solutions for $\Lambda < 1.4$ GeV in the $I(J^P) = \frac{3}{2}(\frac{1}{2})$ configuration. However, the configuration $I(J^P) = \frac{3}{2}(\frac{3}{2})$ with higher isospin and spin is much more difficult to form a bound state. In Fig. 4, one can see that bound-state solutions for $I(J^P) = \frac{3}{2}(\frac{3}{2})$ exist for $\Lambda > 2$ GeV when we scan g_σ and $g_{\sigma NN}$.
2. We also search for bound-state solutions for the $I(J^P) = \frac{3}{2}(\frac{1}{2}^+)$ and $I(J^P) = \frac{3}{2}(\frac{3}{2}^+)$ DD^*N systems when we vary λg_V in the range of 0.5–2.0 times the original value. For the $I(J^P) = \frac{3}{2}(\frac{1}{2}^+)$ configuration, there exist bound-state solutions with a cutoff Λ from about 1.8 to 1.5 GeV. For the $I(J^P) = \frac{3}{2}(\frac{3}{2}^+)$ configuration, we find a bound-state solution with $\Lambda \approx 4.5$ GeV when taking $\lambda g_V = 1.6$ GeV^{-1} (about half of the value in Table I). But we find that the minimum Λ needed for the existence of loosely bound-state solutions in the $I(J^P) = \frac{3}{2}(\frac{3}{2}^+)$ configuration rapidly decreases to 1.5 GeV when we enlarge λg_V to 6.2 GeV^{-1} (about half of the value in Table I).
3. If we vary h_{VNN} from 10 to 40, the minimum cutoff Λ needed for the existence of bound-state solutions is not sensitive to h_{VNN}. For the $I(J^P) = \frac{3}{2}(\frac{1}{2})$ and $I(J^P) = \frac{3}{2}(\frac{3}{2})$ configurations, bound states exist when the cutoff Λ reaches 1.8 and 2.56 GeV, respectively.

In our scheme, the qualitative conclusions about the DD^*N systems with $I(J^P) = \frac{1}{2}(\frac{1}{2}^+)$ and $I(J^P) = \frac{1}{2}(\frac{3}{2}^+)$ are not changed when we vary the coupling constants g_σ, $g_{\sigma NN}$, λg_V, and h_{vNN}. However, the existence of good $I(J^P) = \frac{3}{2}(\frac{1}{2}^+)$ and $I(J^P) = \frac{3}{2}(\frac{3}{2}^+)$ DD^*N molecular candidates is highly dependent on the coupling constants.

V. SUMMARY

The observations of T_{cc} [18,19], $\Lambda_c(2940)$ [30], and $\Sigma_c(2800)$ [39] have provided us a valuable opportunity to deduce the interactions of DD^*, D^*N, and DN, which makes possible the exploration of the double-charm heptaquark states composed of two charmed mesons and one nucleon.

The present work is dedicated to the study of these kinds of double-charm heptaquark states. Based on the deduced D-$D^{(*)}$ and $D^{(*)}$-N effective potentials, we adopted the Gaussian expansion method to solve the three-body Schrödinger equations of the DD^*N system. We searched for bound-state solutions of the DD^*N system, with both S-D mixing and coupled-channel effects considered. Our results imply that the DD^*N bound states with $I(J^P) = \frac{1}{2}(\frac{1}{2}^+)$ and $I(J^P) = \frac{1}{2}(\frac{3}{2}^+)$ are good molecular candidates. On the other hand, the DD^*N systems with $I(J^P) = \frac{3}{2}(\frac{1}{2}^+)$ and $I(J^P) = \frac{3}{2}(\frac{3}{2}^+)$ are difficult to form bound states. The possible decay modes, which can be searched for these predicted DD^*N molecular states, include (a) the $T_{cc}p$ channel, (b) the channels of DDp associated with pions and photons, (c) the channel of Ξ_{cc} with pions, and (d) the channel of a charmed baryon with a charmed meson.

In the past years, the LHCb Collaboration observed many heavy flavor hadronic states including the P_c states [1,2], $P_{cs}(4459)$ [65], $X_{0,1}(2900)$ [66,67], and $X(6900)$ [68]. There is no doubt that the LHCb Collaboration has potential in searching for double-charm heptaquark states predicted in this work, especially with the running of the high-luminosity LHC.

In addition to the DD^*N systems dedicated in this work, we also noticed that some theoretical groups investigated the $\bar{D}^*\bar{D}^{(*)}N$, $B^*B^{(*)}N$, $\bar{D}^{(*)}NN$, and $B^{(*)}NN$ systems [57,69,70], which have different quark components from the discussed DD^*N system in this work. Obviously, the

present work associated with these studies [57,69,70] may reflect the aspect of the three-body hadronic molecular states composed of nucleon and charmed/bottom meson. In future, exploring three-body hadronic molecular states will still be an interesting research topic.

ACKNOWLEDGMENTS

This work is supported by the National Natural Science Foundation of China under Grants No. 11735003, No. 11975041, and No. 11961141004 and the fundamental Research Funds for the Central Universities. X. L. would like to thank the support from the China National Funds for Distinguished Young Scientists under Grant No. 11825503, National Key Research and Development Program of China under Contract No. 2020YFA0406400, the 111 Project under Grant No. B20063, and the National Natural Science Foundation of China under Grant No. 12047501.

[1] R. Aaij *et al.* (LHCb Collaboration), Observation of $J/\psi p$ Resonances Consistent with Pentaquark States in $\Lambda_b^0 \to J/\psi K^- p$ Decays, Phys. Rev. Lett. **115**, 072001 (2015).
[2] R. Aaij *et al.* (LHCb Collaboration), Observation of a Narrow Pentaquark State, $P_c(4312)^+$, and of Two-Peak Structure of the $P_c(4450)^+$, Phys. Rev. Lett. **122**, 222001 (2019).
[3] G. Pakhlova *et al.* (Belle Collaboration), Observation of a Near-Threshold Enhancement in the $e^+e^- \to \Lambda_c^+\Lambda_c^-$ Cross Section Using Initial-State Radiation, Phys. Rev. Lett. **101**, 172001 (2008).
[4] P. Adlarson *et al.* (WASA-at-COSY Collaboration), ABC Effect in Basic Double-Pionic Fusion—Observation of a New Resonance?, Phys. Rev. Lett. **106**, 242302 (2011).
[5] P. Adlarson *et al.* (WASA-at-COSY Collaboration), Abashian-Booth-Crowe resonance structure in the double pionic fusion to He-4, Phys. Rev. C **86**, 032201 (2012).
[6] P. Adlarson *et al.* (WASA-at-COSY Collaboration), Measurement of the $pn \to pp\pi^0\pi^-$ reaction in search for the recently observed resonance structure in $d\pi^0\pi^0$ and $d\pi^+\pi^-$ systems, Phys. Rev. C **88**, 055208 (2013).
[7] P. Adlarson *et al.* (WASA-at-COSY Collaboration), Evidence for a New Resonance from Polarized Neutron-Proton Scattering, Phys. Rev. Lett. **112**, 202301 (2014).
[8] P. Adlarson *et al.* (WASA-at-COSY Collaboration), ABC effect and resonance structure in the double-pionic fusion to ^{3}He, Phys. Rev. C **91**, 015201 (2015).
[9] P. Adlarson *et al.* (WASA-at-COSY Collaboration), Measurement of the $np \to np\pi^0\pi^0$ reaction in search for the recently observed $d^*(2380)$ resonance, Phys. Lett. B **743**, 325 (2015).
[10] H. X. Chen, W. Chen, X. Liu, and S. L. Zhu, The hidden-charm pentaquark and tetraquark states, Phys. Rep. **639**, 1 (2016).
[11] X. Liu, An overview of XYZ new particles, Chin. Sci. Bull. **59**, 3815 (2014).
[12] C. Z. Yuan, The XYZ states revisited, Int. J. Mod. Phys. A **33**, 1830018 (2018).
[13] S. L. Olsen, T. Skwarnicki, and D. Zieminska, Nonstandard heavy mesons and baryons: Experimental evidence, Rev. Mod. Phys. **90**, 015003 (2018).
[14] F. K. Guo, C. Hanhart, U. G. Meißner, Q. Wang, Q. Zhao, and B. S. Zou, Hadronic molecules, Rev. Mod. Phys. **90**, 015004 (2018).
[15] A. Hosaka, T. Iijima, K. Miyabayashi, Y. Sakai, and S. Yasui, Exotic hadrons with heavy flavors: X, Y, Z, and related states, Prog. Theor. Exp. Phys. **2016**, 062C01 (2016).
[16] N. Brambilla, S. Eidelman, C. Hanhart, A. Nefediev, C. P. Shen, C. E. Thomas, A. Vairo, and C. Z. Yuan, The XYZ states: Experimental and theoretical status and perspectives, Phys. Rep. **873**, 1 (2020).
[17] H. X. Chen, W. Chen, X. Liu, Y. R. Liu, and S. L. Zhu, An updated review of the new hadron states, arXiv:2204.02649.
[18] R. Aaij *et al.* (LHCb Collaboration), Observation of an exotic narrow doubly charmed tetraquark, Nat. Phys. **18**, 751 (2022).
[19] R. Aaij *et al.* (LHCb Collaboration), Study of the doubly charmed tetraquark T_{cc}^+, Nat. Commun. **13**, 3351 (2022).
[20] N. Li, Z. F. Sun, X. Liu, and S. L. Zhu, Perfect DD^* molecular prediction matching the T_{cc} observation at LHCb, Chin. Phys. Lett. **38**, 092001 (2021).
[21] H. Ren, F. Wu, and R. Zhu, Hadronic molecule interpretation of T_{cc}^+ and its beauty partners, Adv. High Energy Phys. **2022**, 910303 (2022).
[22] R. Chen, Q. Huang, X. Liu, and S. L. Zhu, Predicting another doubly charmed molecular resonance $T_{cc}'^+(3876)$, Phys. Rev. D **104**, 114042 (2021).
[23] L. R. Dai, R. Molina, and E. Oset, Prediction of new T_{cc} states of D^*D^* and $D_s^*D^*$ molecular nature, Phys. Rev. D **105**, 016029 (2022).
[24] A. Feijoo, W. H. Liang, and E. Oset, $D^0D^0\pi+$ mass distribution in the production of the T_{cc} exotic state, Phys. Rev. D **104**, 114015 (2021).
[25] T. W. Wu, Y. W. Pan, M. Z. Liu, S. Q. Luo, L. S. Geng, and X. Liu, Discovery of the doubly charmed T_{cc}^+ state implies a triply charmed H_{ccc} hexaquark state, Phys. Rev. D **105**, L031505 (2022).
[26] R. Molina, T. Branz, and E. Oset, A new interpretation for the $D_{s2}^*(2573)$ and the prediction of novel exotic charmed mesons, Phys. Rev. D **82**, 014010 (2010).
[27] N. Li, Z. F. Sun, X. Liu, and S. L. Zhu, Coupled-channel analysis of the possible $D^{(*)}D^{(*)}$, $\bar{B}^{(*)}\bar{B}^{(*)}$ and $D^{(*)}\bar{B}^{(*)}$ molecular states, Phys. Rev. D **88**, 114008 (2013).

[28] M. Z. Liu, T. W. Wu, M. Pavon Valderrama, J. J. Xie, and L. S. Geng, Heavy-quark spin and flavor symmetry partners of the $X(3872)$ revisited: What can we learn from the one boson exchange model?, Phys. Rev. D **99**, 094018 (2019).

[29] H. Xu, B. Wang, Z. W. Liu, and X. Liu, DD^* potentials in chiral perturbation theory and possible molecular states, Phys. Rev. D **99**, 014027 (2019).

[30] B. Aubert *et al.* (*BABAR* Collaboration), Observation of a Charmed Baryon Decaying to D^0p at a Mass near 2.94 GeV/c^2, Phys. Rev. Lett. **98**, 012001 (2007).

[31] K. Abe *et al.* (Belle Collaboration), Experimental Constraints on the Possible J^P Quantum Numbers of the $\Lambda_c(2880)^+$, Phys. Rev. Lett. **98**, 262001 (2007).

[32] R. Aaij *et al.* (LHCb Collaboration), Study of the D^0p amplitude in $\Lambda_b^0 \to D^0p\pi^-$ decays, J. High Energy Phys. 05 (2017) 030.

[33] X. G. He, X. Q. Li, X. Liu, and X. Q. Zeng, $\Lambda_c^+(2940)$: A possible molecular state?, Eur. Phys. J. C **51**, 883 (2007).

[34] Y. Dong, A. Faessler, T. Gutsche, S. Kumano, and V. E. Lyubovitskij, Radiative decay of $\Lambda_c(2940)^+$ in a hadronic molecule picture, Phys. Rev. D **82**, 034035 (2010).

[35] J. He, Y. T. Ye, Z. F. Sun, and X. Liu, The observed charmed hadron $\Lambda_c(2940)^+$ and the D^*N interaction, Phys. Rev. D **82**, 114029 (2010).

[36] P. G. Ortega, D. R. Entem, and F. Fernandez, The $\Lambda_c(2940)^+$ as a D^*N molecule in a constituent quark model and a possible $\Lambda_b(6248)$, Few-Body Syst. **54**, 1101 (2013).

[37] B. Wang, L. Meng, and S. L. Zhu, $D^{(*)}N$ interaction and the structure of $\Sigma_c(2800)$ and $\Lambda_c(2940)$ in chiral effective field theory, Phys. Rev. D **101**, 094035 (2020).

[38] S. Q. Luo, B. Chen, Z. W. Liu, and X. Liu, Resolving the low mass puzzle of $\Lambda_c(2940)^+$, Eur. Phys. J. C **80**, 301 (2020).

[39] R. Mizuk *et al.* (Belle Collaboration), Observation of an Isotriplet of Excited Charmed Baryons Decaying to $\Lambda_c^+\pi$, Phys. Rev. Lett. **94**, 122002 (2005).

[40] Z. Y. Wang, J. J. Qi, X. H. Guo, and K. W. Wei, Study of molecular ND bound states in the Bethe-Salpeter equation approach, Phys. Rev. D **97**, 094025 (2018).

[41] J. R. Zhang, S-wave $D^{(*)}N$ molecular states: $\Sigma_c(2800)$ and $\Lambda_c(2940)^+$?, Phys. Rev. D **89**, 096006 (2014).

[42] Y. Dong, A. Faessler, T. Gutsche, and V. E. Lyubovitskij, Charmed baryon $\Sigma_c(2800)$ as a ND hadronic molecule, Phys. Rev. D **81**, 074011 (2010).

[43] E. Hiyama, Gaussian expansion method for few-body systems and its applications to atomic and nuclear physics, Prog. Theor. Exp. Phys. **2012**, 01A204 (2012).

[44] E. Hiyama, Y. Kino, and M. Kamimura, Gaussian expansion method for few-body systems, Prog. Part. Nucl. Phys. **51**, 223 (2003).

[45] R. Chen, A. Hosaka, and X. Liu, Prediction of triple-charm molecular pentaquarks, Phys. Rev. D **96**, 114030 (2017).

[46] P. A. Zyla *et al.* (Particle Data Group Collaboration), Review of particle physics, Prog. Theor. Exp. Phys. **2020**, 083C01 (2020).

[47] T. W. Wu, M. Z. Liu, L. S. Geng, E. Hiyama, and M. P. Valderrama, DK, DDK, and $DDDK$ molecules–understanding the nature of the $D_{s0}^*(2317)$, Phys. Rev. D **100**, 034029 (2019).

[48] T. W. Wu, M. Z. Liu, L. S. Geng, E. Hiyama, M. P. Valderrama, and W. L. Wang, Quadruply charmed dibaryons as heavy quark symmetry partners of the DDK bound state, Eur. Phys. J. C **80**, 901 (2020).

[49] T. W. Wu, M. Z. Liu, and L. S. Geng, Excited K meson, $K_c(4180)$, with hidden charm as a $D\bar{D}K$ bound state, Phys. Rev. D **103**, L031501 (2021).

[50] T. W. Wu, Y. W. Pan, M. Z. Liu, J. X. Lu, L. S. Geng, and X. H. Liu, Hidden charm hadronic molecule with strangeness $P_{cs}^*(4739)$ as a $\Sigma_c\bar{D}\bar{K}$ bound state, Phys. Rev. D **104**, 094032 (2021).

[51] T. W. Wu and L. S. Geng, Study on triple-hadron bound states with gaussian expansion method, Few-Body Syst. **62**, 89 (2021).

[52] T. W. Wu, M. Z. Liu, and L. S. Geng, One way to verify the molecular picture of exotic hadrons: From DK to $DDK/D\bar{D}^{(*)}K$, Few-Body Syst. **62**, 38 (2021).

[53] S. Q. Luo, T. W. Wu, M. Z. Liu, L. S. Geng, and X. Liu, Triple-charm molecular states composed of D^*D^*D and $D^*D^*D^*$, Phys. Rev. D **105**, 074033 (2022).

[54] R. Chen, X. Liu, X. Q. Li, and S. L. Zhu, Identifying Exotic Hidden-Charm Pentaquarks, Phys. Rev. Lett. **115**, 132002 (2015).

[55] R. Chen, Z. F. Sun, X. Liu, and S. L. Zhu, Strong LHCb evidence supporting the existence of the hidden-charm molecular pentaquarks, Phys. Rev. D **100**, 011502 (2019).

[56] R. Chen, F. L. Wang, A. Hosaka, and X. Liu, Exotic triple-charm deuteronlike hexaquarks, Phys. Rev. D **97**, 114011 (2018).

[57] S. Yasui and K. Sudoh, Exotic nuclei with open heavy flavor mesons, Phys. Rev. D **80**, 034008 (2009).

[58] S. Godfrey and N. Isgur, Mesons in a relativized quark model with chromodynamics, Phys. Rev. D **32**, 189 (1985).

[59] S. Capstick and N. Isgur, Baryons in a relativized quark model with chromodynamics, Phys. Rev. D **34**, 2809 (1986).

[60] F. L. Wang and X. Liu, Investigating new type of doubly charmed molecular tetraquarks composed of charmed mesons in the H and T doublets, Phys. Rev. D **104**, 094030 (2021).

[61] F. L. Wang, X. D. Yang, R. Chen, and X. Liu, Correlation of the hidden-charm molecular tetraquarks and the charmoniumlike structures existing in the $B \to XYZ + K$ process, Phys. Rev. D **104**, 094010 (2021).

[62] X. D. Yang, F. L. Wang, Z. W. Liu, and X. Liu, Newly observed X(4630): A new charmoniumlike molecule, Eur. Phys. J. C **81**, 807 (2021).

[63] F. L. Wang, X. D. Yang, R. Chen, and X. Liu, Hidden-charm pentaquarks with triple strangeness due to the $\Omega_c^{(*)}\bar{D}_s^{(*)}$ interactions, Phys. Rev. D **103**, 054025 (2021).

[64] R. Aaij *et al.* (LHCb Collaboration), Observation of the Doubly Charmed Baryon Ξ_{cc}^{++}, Phys. Rev. Lett. **119**, 112001 (2017).

[65] R. Aaij *et al.* (LHCb Collaboration), Evidence of a $J/\psi\Lambda$ structure and observation of excited Ξ^- states in the $\Xi_b^- \to J/\psi\Lambda K^-$ decay, Sci. Bull. **66**, 1278 (2021).

[66] R. Aaij *et al.* (LHCb Collaboration), A Model-Independent Study of Resonant Structure in $B^+ \to D^+D^-K^+$ Decays, Phys. Rev. Lett. **125**, 242001 (2020).

[67] R. Aaij *et al.* (LHCb Collaboration), Amplitude analysis of the $B^+ \to D^+D^-K^+$ decay, Phys. Rev. D **102**, 112003 (2020).

[68] R. Aaij *et al.* (LHCb Collaboration), Observation of structure in the J/ψ -pair mass spectrum, Sci. Bull. **65**, 1983 (2020).

[69] H. Garcilazo, A. Valcarce, and T. F. Caramés, Three-body systems with open flavor heavy mesons, Phys. Rev. D **96**, 074009 (2017).

[70] Y. Yamaguchi, S. Yasui, and A. Hosaka, Exotic dibaryons with a heavy antiquark, Nucl. Phys. **A927**, 110 (2014).